

Peroxidase-like activity of photochromic PVP-stabilized tungsten oxide nanoparticles: assessment by independent chemiluminescent and colorimetric assays

Matvei A. Popkov^{1,a}, Ekaterina D. Sheichenko^{1,2,b}, Arina D. Filippova^{1,c}, Ilya V. Tronev^{1,2,d}, Kristina N. Novoselova^{1,2,e}, Evelina A. Trufanova^{1,2,f}, Darya N. Vasilyeva^{1,2,g}, Maria R. Protsenko^{1,2,h}, Madina M. Sozarukova^{1,j}, Alexander E. Baranchikov^{1,2,k}, Vladimir K. Ivanov^{1,2,l}

¹Kurnakov Institute of General and Inorganic Chemistry, Russian Academy of Sciences, Moscow, Russia

²HSE University, Moscow, Russia

^ama_popkov@igic.ras.ru, ^bedsheychenko@edu.hse.ru, ^carifilippova@yandex.ru, ^divtronev@edu.hse.ru,

^eknnovoselova@edu.hse.ru, ^featrufanova_1@edu.hse.ru, ^gDnvasileva_1@edu.hse.ru,

^hmrprotsenko@edu.hse.ru, ^js_madinam@bk.ru, ^ka.baranchikov@yandex.ru, ^lvan@igic.ras.ru

Corresponding author: M. A. Popkov, ma_popkov@igic.ras.ru

PACS 68.65.-k, 78.67.-n, 82.65.+r

ABSTRACT In this work, peroxidase-like activity of ultrasmall tungsten oxide nanoparticles including those stabilized with polyvinylpyrrolidone (PVP) was assessed using two independent approaches: the colorimetric method, which is based on the analysis of 3,3',5,5'-tetramethylbenzidine (TMB) oxidation, and the luminol-enhanced chemiluminescence method. It was demonstrated that bare tungsten oxide nanoparticles effectively catalyze the decomposition of hydrogen peroxide. In turn, the PVP-stabilized nanoparticles possess lower catalytic activity, which can be attributed to a decrease in the number of available active centres on the nanoparticle surface.

KEYWORDS nanomaterials, nanozymes, sols, photochromic materials, chemiluminescence, TMB, peroxidase-like activity.

ACKNOWLEDGEMENTS The publication was prepared within the framework of the Academic Fund Program at HSE University (grant 24-00-036, Enzyme-like activity of nanodispersed inorganic materials). The studies were carried out on the equipment of the Joint Scientific Center for Physical Research Methods of the Kurnakov Institute of General and Inorganic Chemistry of the Russian Academy of Sciences, Moscow, Russia.

FOR CITATION Popkov M.A., Sheichenko E.D., Filippova A.D., Tronev I.V., Novoselova K.N., Trufanov E.A., Vasilyeva D.N., Protsenko M.R., Sozarukova M.M., Baranchikov A.E., Ivanov V.K. Peroxidase-like activity of photochromic PVP-stabilized tungsten oxide nanoparticles: assessment by independent chemiluminescent and colorimetric assays. *Nanosystems: Phys. Chem. Math.*, 2025, **16** (1), 22–29.

1. Introduction

In recent years, it has been demonstrated that certain inorganic nanomaterials are capable of participating in biochemical processes, performing functions analogous to those of natural enzymes [1, 2]. Such materials have been identified as a distinct class called nanozymes. Among them, nanoparticles of transition and rare earth metal oxides with switchable redox state are of particular interest. A number of studies have demonstrated that nanoscale oxide nanoparticles, including Fe₃O₄ [3, 4], CeO₂ [5–7], MnO₂ [8], and TiO₂ [9], exhibit oxidoreductase-like activity rendering them perspective regulators of free-radical reactions or even redox-metabolism in cells. Extended insights into enzyme-mimetic properties of inorganic nanoparticles could facilitate their application in both medical and ecological contexts.

One of the materials exhibiting high redox activity is tungsten oxide nanoparticles [10]. WO₃ is a semiconductor material demonstrating photochromic, electrochromic and photocatalytic properties [11–14]. Tungsten oxide nanoparticles effectively absorb ultraviolet radiation being able to show reversible coloring-bleaching cycles as a result of partial reduction of W⁺⁶ and oxidation of W⁺⁴/W⁺⁵ states [15, 16]. Oxidants, such as NO₂ or H₂O₂, can also facilitate the redox transitions of tungsten ions, thus tungsten oxides can act as probes for these species [17, 18]. The coordination of WO₃ nanoparticles with OH- or NH₂-groups of certain organic stabilizers has been demonstrated to enhance the rate of the redox transitions, to intensify the color changes and to facilitate the cycling of coloration-decoloration processes [19].

WO₃-based materials have gained considerable attention as coatings for electrochemical sensors used for the detection of gases [14, 20] and biomolecules [21, 22]. It has been demonstrated that tungsten oxide possesses antibacterial and antifungal properties, being selectively toxic to human cancer cells [23–25]. This issue paves the way for new applications of tungsten oxide nanomaterials in medicine, including healing and disinfecting of wounds.

Recent research has demonstrated that nanoscale tungsten oxide is able to catalyze the decomposition of hydrogen peroxide, thus performing similar to the natural enzyme –peroxidase [26, 27]. This fact broadens the understanding of the biochemical activity of tungsten oxide nanoparticles, facilitating their consideration as a potential theranostic agent. However, the recent criticism on the probing the enzyme-like activities of inorganic nanoparticles [28, 29] challenges their extended analysis by independent analytical methods including the use of classic enzyme kinetic modeling for the correct assessment of the biocatalytic characteristics of nanomaterials.

Our previous report demonstrated that photochromic tungsten oxide nanoparticles, obtained by ion exchange from sodium tungstate, probably catalyze the decomposition of hydrogen peroxide [19]. In this study, we focused on this effect and investigated the possible peroxidase-like activity of ultrasmall WO_x particles by two independent assays: colorimetric assay using 3,3',5,5'-tetramethylbenzidine; and chemiluminescence analysis of luminol oxidation by hydrogen peroxide.

2. Materials and methods

2.1. Synthesis and characterization of tungsten oxide nanoparticles

Ultrasmall tungsten oxide nanoparticles were prepared by ion-exchange method [11] using Na_2WO_4 (Rushim, CAS 10213-10-2) solution and strongly acidic cation exchange resin (Amberlite, IR120). Briefly, the ion exchange resin in protonated form was placed in a separating funnel (filling volume 100 mL), then 50 mL of 20 mM sodium tungstate solution was passed through this column. The obtained colloid solution was divided into two parts. To the first, 0.67 g of polyvinylpyrrolidone (PVP k-30, Sigma, CAS 9003-39-8) was added, the sol was transferred to a flask and stirred for 4 h at 90 °C. After stabilization, a clear colloidal solution of WO_x was obtained. The second part was used as synthesized.

To determine the possible effect of the stabilizer (PVP) on the peroxidase-like activity, we prepared 40 mM PVP aqueous solution (control).

Powder X-ray diffraction (XRD) patterns were collected using Bruker D8 Advance diffractometer (USA) with $CuK\alpha$ -radiation in the 2θ range of 5–50° with a step of 0.02° and counting time at least of 0.2 s per step.

Analysis of particle size distribution by dynamic light scattering (DLS) and ζ -potential measurements were carried out using a Photocor Compact-Z analyzer (Russia) equipped with a 636.65 nm laser at 20 °C. The correlation function for each sample was obtained by averaging 10 curves, each of which was accumulated for 20 s. The hydrodynamic radius of aggregates was determined by the regularization method using DynalS software.

FTIR-spectra were recorded in the wavenumber range of 400–4,000 cm^{-1} with a spectral resolution of 2 cm^{-1} using an InfraLUM FT-08 infrared spectrometer (Russia).

The optical absorption spectra were recorded using quartz cuvettes (10.0 mm optical path length) in a 200–600 nm range, at 0.1 nm steps, on an SF-2000 spectrophotometer (Russia) with a deuterium-halogen light source.

2.2. Analysis of peroxidase-like property by luminol-enhanced chemiluminescence method

The peroxidase-like activity of the WO_x sols was investigated using the chemiluminescent method which is based on the registration of luminol oxidation by hydrogen peroxide in a phosphate buffer solution (100 mM, pH 7.4) at 37 °C. Luminol (5-amino-1,2,3,4-tetrahydro-1,4-phthalazindione, Sigma 123072) and hydrogen peroxide (Aldosa, CAS 7722-84-1) were added to the buffer solution sequentially until concentrations of 50 μ M and 10 mM were reached, respectively. Chemiluminescence signal was recorded in 2 ml plastic cuvettes using a 12-channel chemiluminometer DISoft Lum-1200 (Russia) and analyzed using the PowerGraph software v.3.3 (Russia).

2.3. Analysis of peroxidase-like property by colorimetric method

Peroxidase-like activity was investigated by the reaction of TMB (3,3',5,5'-tetramethylbenzidine hydrochloride, Sigma 87750) oxidation by hydrogen peroxide in an acetate buffer (0.2 M, pH 4.00) at 37 °C.

A solution of TMB (40 mM, 0–150 μ l) in an aqueous solution of 6M acetic acid, and hydrogen peroxide (2 M, 37.5 μ l) were added sequentially to the buffer solution. The mixture was incubated at 37 °C for 2 min, then WO_x sol (20 mM, 75 μ l) was added. The total volume of the mixture was 1.5 ml. The coloration (from colorless to blue) kinetics of the obtained solution was recorded every 2 sec for 5 min in the wavelength range of 450–800 nm with a step of 1 nm using an Ocean Optics QE65000 spectrometer (USA) using an HPX-2000 xenon lamp equipped with a 450 nm UV-filter.

3. Results and discussion

Transparent sols of tungsten oxide nanoparticles with or without polyvinylpyrrolidone (PVP) as a stabilizing agent were obtained using an ion exchange technique. The concentration of the sols was measured gravimetrically to be 20.4 and 19.6 mM, respectively.

The particle size distribution was determined using dynamic light scattering (Fig. 1a). The unstabilized WO_x nanoparticles demonstrated a monodisperse size distribution, with an average hydrodynamic diameter of 4.8 nm and a ζ -potential of –20 mV. The solution of bare WO_x possessed low aggregation stability and precipitated within 72 h. Thus, all the experiments with this material were performed in few hours after the synthesis (freshly prepared samples). In the WO_x @PVP

sol, three fractions of particles were present with average hydrodynamic diameters of 1.6, 7.3 and 52 nm. The zeta potential of the sol was about -2 mV, while the sol exhibited excellent colloidal stability (more than several months) indicating the steric stabilization by a polymer layer.

Fig. 1b shows the diffraction pattern of the dried tungsten oxide sol stabilized by PVP. The material is mostly amorphous, the observed broad peak in the small angle region ($2\theta < 10^\circ$) can be attributed to the scattering on ultrasmall WO_x nanoparticles according to the previous reports [11, 30].

The IR spectra of the PVP powder and the dried WO_x @PVP sol are shown in Fig. 1c-d. Both spectra show absorption bands related to characteristic vibrations of polyvinylpyrrolidone. The absorption bands of O–H stretching vibrations overlap with the absorption band of N–H stretching vibrations of PVP, forming a wide band in the region of $3,500$ – $3,100$ cm^{-1} . The bands corresponding to stretching and bending vibrations of CH_2 group are observed in the regions of $2,900$ cm^{-1} and $1,300$ – $1,200$ cm^{-1} , respectively. Bands in the region $1,480$ – $1,390$ cm^{-1} were attributed to the N–C stretching vibrations. The absorption bands in the region of 500 – $1,000$ cm^{-1} refer to skeletal vibrations of PVP: (C–C) 933 cm^{-1} , $\delta(\text{CH}_2)$ 843 cm^{-1} , $\delta(\text{N–C=O})$ 648 cm^{-1} , 574 cm^{-1} . The IR spectrum of the dried WO_x @PVP sol also shows absorption bands related to the valence vibrations of WO_3 bonds (W=O) 955 cm^{-1} , (O–W–O) 820 cm^{-1} , 795 cm^{-1} , which agrees well with the recently reported data [30, 31].

The WO_x @PVP sols exhibit a rapid change in color from transparent to blue under UV irradiation, due to the reduction of W^{+6} by PVP [32]. Such a reduction mechanism was also observed in heteropolynuclear molybdenum complexes with PVP under UV irradiation [33]. Fig. 2 shows photographs and UV-visible spectra of the WO_x @PVP sol before and after 30 sec of UV irradiation at 365 nm. The UV-vis spectrum of the irradiated sol shows a broad absorption band with a maximum at 630 nm, corresponding to reduced tungsten oxide species. The mechanism of reduction was discussed recently [11, 19]. It should be noted that the unstabilized sol does not demonstrate any coloration even after prolonged irradiation (more than 20 min). It can be concluded that upon interaction of tungsten oxide nanoparticles with PVP, a complex with charge transfer is formed which promotes the reduction of tungsten ions and slows down their further oxidation in aqueous solution.

The peroxidase-like activity of both tungsten oxide sols was investigated using chemiluminescence method, with luminol as a probe molecule. The experiments were carried out in a 0.1 M phosphate buffer solution (pH 7.4) at 37 °C. The decomposition of hydrogen peroxide results in the formation of hydroxyl radicals, which are capable of oxidizing luminol, thereby yielding luminescence signal. The nanoparticles can affect the decomposition process thus enhancing the chemiluminescence, which could be used to assess their catalytic activity.

Fig. 3(a–c) shows the chemiluminescence curves after the addition of WO_x @PVP or the bare WO_x sol or PVP solution to luminol-hydrogen peroxide mixture. As can be seen from the Fig. 3a, the addition of WO_x @PVP sol at concentrations of 10.2 – 510 μM to the solution increases the luminescence intensity in a dose-dependent manner. It can be concluded that upon the increase in the concentration of the catalyst, the rate of ROS generation increases, too.

In turn, the addition of bare WO_x nanoparticles to the reaction mixture results in a short increase in the intensity of the luminescence, which can be attributed to the very fast generation of hydroxyl radicals (Fig. 3b). After an initial flash-like stage, the luminescence intensity descends to a stationary level in approximately three minutes. It is reasonable to assume that the observed burst of luminescence is due to the high amount of the reaction centres on the nanoparticles' surface.

To confirm that it is the WO_x nanoparticles that exhibit peroxidase-like activity, the luminescence kinetics of luminol was recorded upon addition of a PVP solution in the concentration range 10 μM – 8 mM. Fig. 3c shows that the addition of PVP results only in a slight increase in luminol-associated luminescence intensity, which indicates the absence of any catalytic activity inherent in the polymer.

The integral chemiluminescence intensity (Fig. 3d) shows a dose-dependent correlation of the rate of hydrogen peroxide decomposition in the presence of the tungsten oxide nanoparticles in the concentration range of 10.2 – 510 μM . In addition, the integral luminol luminescence intensity upon addition of the bare WO_x sol is nearly 10 times higher compared to the PVP-stabilized WO_x sol.

The peroxidase-like activity of nanoparticles is often determined by the colorimetric method using standard substrates such as hydrogen peroxide and 3,3',5,5'-tetramethylbenzidine (TMB) [34]. The catalyst accelerates the homolytic fission of the O–O bond in hydrogen peroxide, resulting in the generation of free hydroxyl radicals. The rate of radical generation is directly proportional to the rate of oxidation of TMB, which is converted to the colored (absorption at 652 nm) cation-radical form by a one-electron process. The corresponding reaction is typically conducted in a buffer solution at pH 3–6. The optimal pH value is approximately 4, and the ionic strength of the buffer is 0.1 – 0.2 M [35]. Here, we should emphasize that, in our experiments, the chemiluminescence and colorimetric measurements were conducted at different pH, ~ 7 for chemiluminescence and ~ 4 for colorimetric. This difference is due to very low luminescence intensity of luminol oxidation product (aminophthalic acid) at $\text{pH} < 6$ and low rate of TMB coloration at $\text{pH} > 6$. The rate of decomposition of hydrogen peroxide varies with pH [36, 37], but the underlying reaction mechanism is pH-independent, thereby permitting a qualitative comparison of the two analytical methods.

The colorimetric experiments were carried out in a 0.2 M acetate buffer solution (pH 4.00) at a temperature of 37 °C. The decomposition of hydrogen peroxide results in the formation of hydroxyl radicals, which are capable of oxidizing

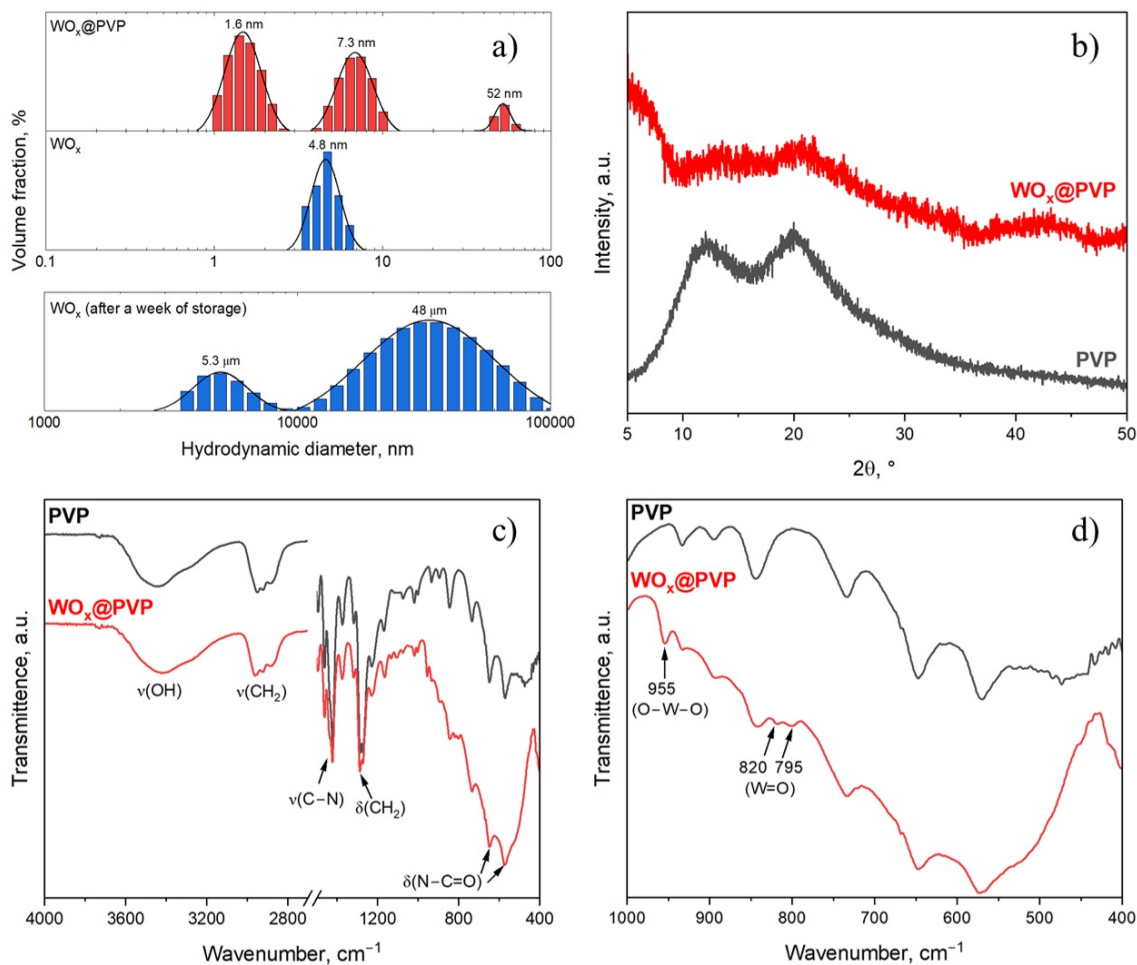


FIG. 1. (a) Hydrodynamic diameter distributions for the WO_x@PVP sol, bare WO_x sol immediately after the synthesis and after a week of storage under ambient conditions; (b) X-ray diffraction patterns of the dried WO_x@PVP sol and PVP powder; (c-d) FTIR spectra of PVP and WO_x@PVP powders

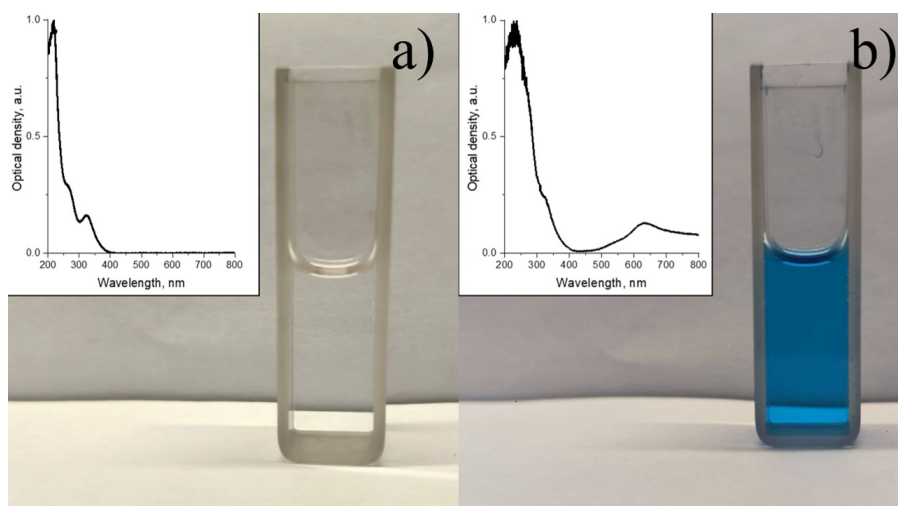


FIG. 2. Photographs and UV-vis spectra of WO_x@PVP sols (a) before and (b) after 30 s of the UV-irradiation (λ = 365 nm)

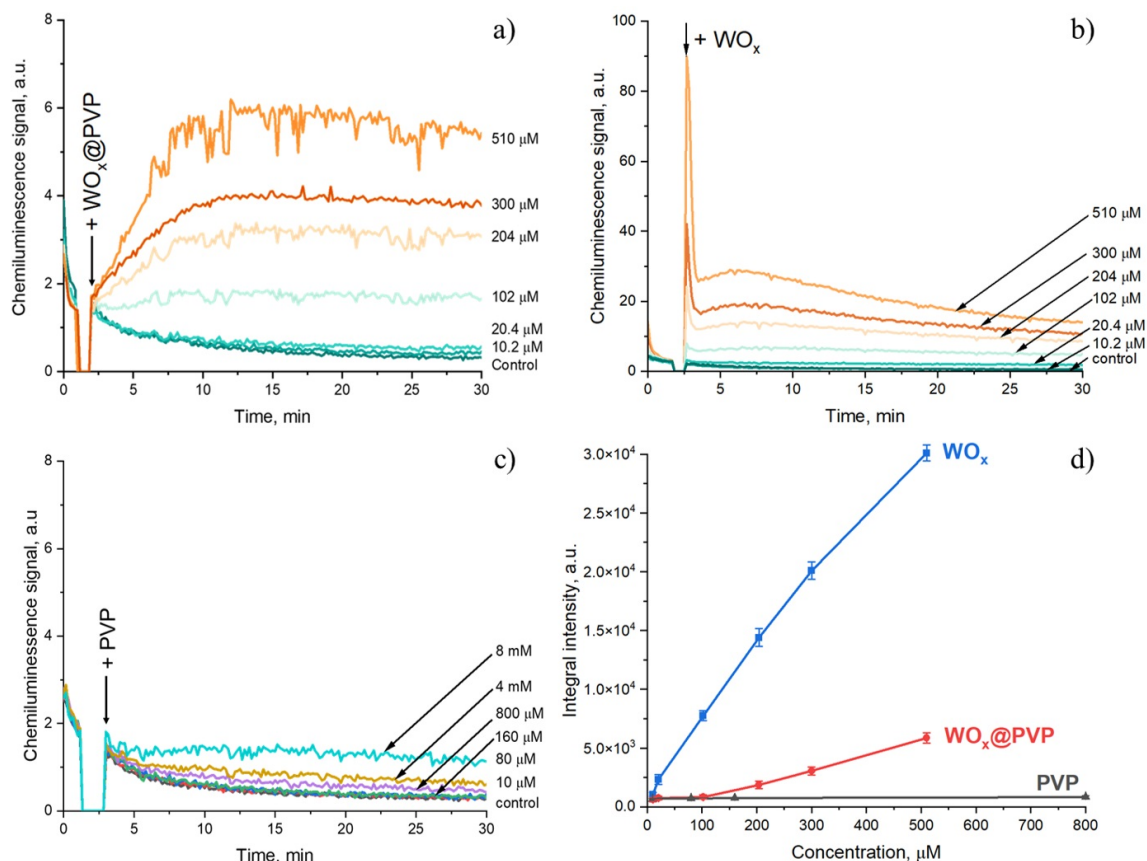


FIG. 3. Chemiluminescence kinetic curves for the H_2O_2 /luminol solutions upon addition of (a) WO_x @PVP sol (10.2 – 510 μM), (b) bare WO_x sol (10.2 – 510 μM) and (c) PVP aqueous solution (10 μM – 8 mM). The experimental data were obtained via direct chemiluminescent measurements. Control: luminol and H_2O_2 in a phosphate-buffered solution without WO_x and/or PVP. (d) The integral luminescence intensities of the reaction mixtures measured within 20 min after the addition of a tested material

TMB, thereby causing its coloration. The incorporation of nanoparticles into the mixture may result in an enhancement of coloration, which would demonstrate their catalytic activity. The UV-visible absorption spectra of the reaction mixture were recorded at 2-second intervals, and the time dependence of the absorption intensity at 652 nm (the wavelength of maximum absorption of the colored oxidation product of TMB) was determined (Fig. 4). To eliminate the influence of ultraviolet radiation on redox processes at the surface of tungsten oxide nanoparticles, a light filter was installed in front of the reaction mixture to block radiation with a wavelength shorter than 450 nm.

Bare WO_x nanoparticles demonstrated dose-dependent catalytic activity in the hydrogen peroxide decomposition reaction. In turn, the activity of WO_x @PVP sols at the same concentration range is approximately 10–20 times lower than the catalytic activity of the bare nanoparticles. These data are in good accordance with the results of the chemiluminescence analysis.

The time dependencies of the optical density of the reaction mixture (proportional to the concentration of the oxidized form of TMB) containing the bare WO_x nanoparticles (Fig. 5) were found to be fitted well to the Michaelis-Menten equation

$$\nu = \frac{V_{MAX} \cdot [S]}{K_M + [S]}$$

where ν is the initial reaction rate, V_{MAX} is the maximum reaction rate, and K_M is the Michaelis constant, which reflects the affinity of a catalyst for the substrate, and $[S]$ is the substrate (TMB) concentration. The correspondence of the kinetics of substrate oxidation in the presence of inorganic nanoparticles to the Michaelis-Menten model confirms their enzyme-like activity.

The following kinetic parameters were determined from the Michaelis-Menten equation ($R^2 > 0.99$). The Michaelis constant was found to be $(3.9 \pm 0.5) \times 10^{-3}$ M, the maximum reaction rate was determined to be $(1.5 \pm 0.2) \times 10^{-7}$ $\text{M}\cdot\text{s}^{-1}$. The catalytic constant (k_{cat}) is the rate constant defining the maximum number of substrate molecules undergoing transformation per time unit. The k_{cat} for the WO_x nanocatalyst amounted to $1.5 \cdot 10^{-4}$ s^{-1} . These kinetic parameters are in line with those typically reported for various inorganic nanoparticles [38–40].

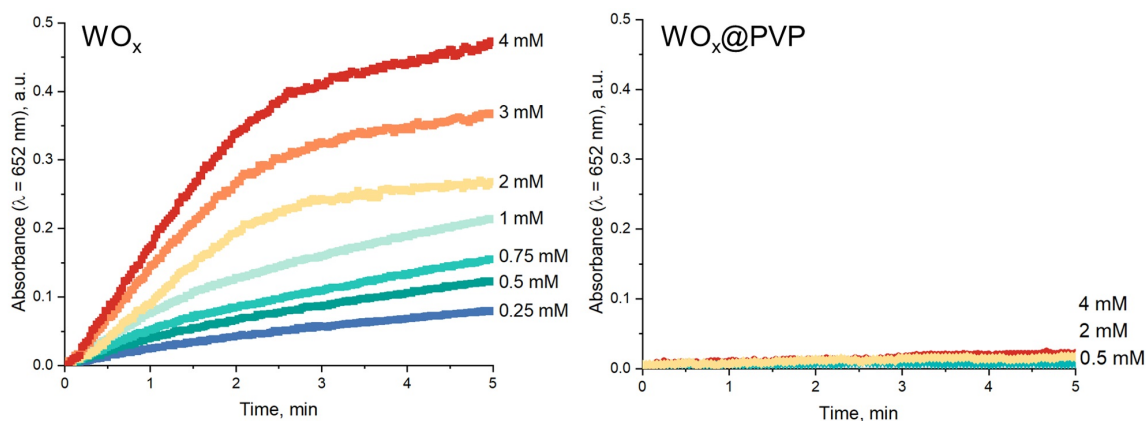


FIG. 4. The kinetics of TMB oxidation by hydrogen peroxide in the presence of (a) bare WO_x (0.25–4 mM) and (b) WO_x@PVP (0.5–4 mM) nanoparticles as determined from the absorption at 652 nm.

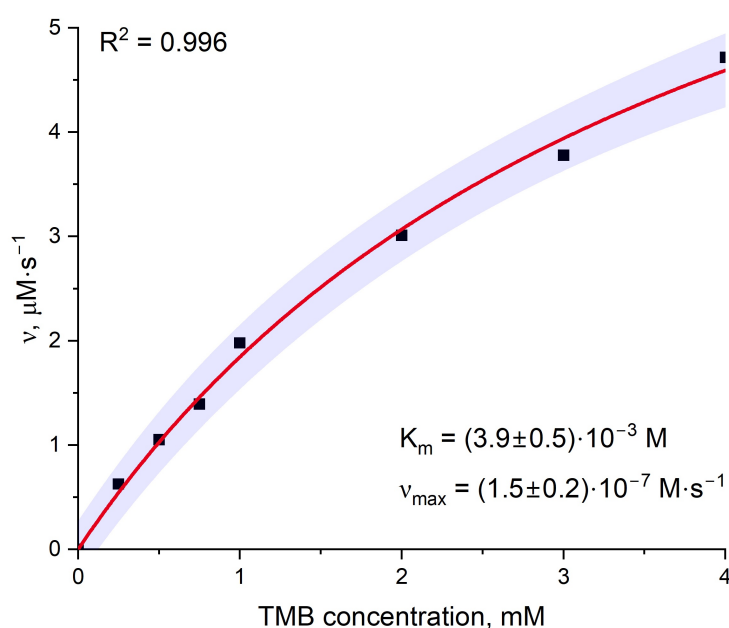


FIG. 5. The kinetics of TMB oxidation by hydrogen peroxide in the presence of bare WO_x sols and its fitting to the Michaelis-Menten model. The light-purple band shows 95 % coincidence interval

A quantitative comparison of the results obtained by chemiluminescent and colorimetric methods is challenging due to the impossibility of constructing a calibration curve which would correlate the rate of hydrogen peroxide decomposition and the chemiluminescence intensity. Additionally, the analytical signal is significantly dependent on the pH of the buffer solution. However, despite these limitations, the both methods demonstrate a high qualitative agreement.

4. Conclusions

Ultra-small non-stabilized and PVP-stabilized tungsten oxide nanoparticles were synthesized by the ion exchange method and their peroxidase-like activity was evaluated using two independent assays: colorimetric and chemiluminescent. The results obtained demonstrate that the bare tungsten oxide nanoparticles exhibited a dose-dependent catalytic activity. The oxidation of 3,3',5,5'-tetramethylbenzidine (TMB) by hydrogen peroxide in the presence of the nanoparticles is described by the Michaelis-Menten model. The calculated kinetic parameters were $K_S = (3.9 \pm 0.5) \times 10^{-3}$ M, $V_{MAX} = (1.5 \pm 0.2) \times 10^{-7}$ M·s⁻¹ M·s⁻¹ and $k_{cat} = 1.5 \cdot 10^{-4}$ s⁻¹.

The stabilization of the WO_x nanoparticles with PVP substantially decreases their peroxidase-like activity, which is 10–20 times lower than the catalytic activity of the bare WO_x nanoparticles. This behavior may be attributed to a shielding of the available active sites on the nanoparticles surface.

References

- [1] Kang T., Kim Y.G., Kim D., Hyeon T. Inorganic nanoparticles with enzyme-mimetic activities for biomedical applications. *Coord. Chem. Rev.*, 2020, **403**, P. 213092.
- [2] Liang X., Han L. White Peroxidase-Mimicking Nanozymes: Colorimetric Pesticide Assay without Interferences of O₂ and Color. *Adv. Funct. Mater.*, 2020, **30**(28), P. 2001933.
- [3] Gao L., Zhuang J., Nie L., et al. Intrinsic peroxidase-like activity of ferromagnetic nanoparticles. *Nat. Nanotechnol.*, 2007, **2**(9), P. 577–583.
- [4] Gao L. Enzyme-Like Property (Nanozyme) of Iron Oxide Nanoparticles. In: *Iron Oxide Nanoparticles*, IntechOpen, 2022.
- [5] Yang Y., Mao Z., Huang W., et al. Redox enzyme-mimicking activities of CeO₂ nanostructures: Intrinsic influence of exposed facets. *Sci. Rep.*, 2016, **6**(1), P. 35344.
- [6] Filippova A.D., Baranchikov A.E., Ivanov V.K. Enzyme-Like Activity of Cerium Dioxide Colloidal Solutions Stabilized with L-Malic Acid. *Colloid. J.*, 2023, **85**(5), P. 782–794.
- [7] Filippova A.D., Sozarukova M.M., Baranchikov A.E., Kottsov S.Y., Cherednichenko K.A., Ivanov V.K. Peroxidase-like Activity of CeO₂ Nanozymes: Particle Size and Chemical Environment Matter. *Molecules*, 2023, **28**(9), P. 3811.
- [8] Zhao M., Tao Y., Huang W., He Y. Reversible pH switchable oxidase-like activities of MnO₂ nanosheets for a visual molecular majority logic gate. *Phys. Chem. Chem. Phys.*, 2018, **20**(45), P. 28644–28648.
- [9] Lin S., Tan W., Han P., et al. A photonanozyme with light-empowered specific peroxidase-mimicking activity. *Nano. Res.*, 2022, **15**(10), P. 9073–9081.
- [10] Deng Z., Gong Y., Luo Y., Tian Y. WO₃ nanostructures facilitate electron transfer of enzyme: Application to detection of H₂O₂ with high selectivity. *Biosens. Bioelectron.*, 2009, **24**(8), P. 2465–2469.
- [11] Kozlov D.A., Shcherbakov A.B., Kozlova T.O., et al. Photochromic and Photocatalytic Properties of Ultra-Small PVP-Stabilized WO₃ Nanoparticles. *Molecules*, 2019, **25**(1), P. 154.
- [12] Lee S.-H., Deshpande R., Parilla P.A., et al. Crystalline WO₃ Nanoparticles for Highly Improved Electrochromic Applications. *Adv. Mater.*, 2006, **18**(6), P. 763–766.
- [13] Aliannezhadi M., Abbaspoor M., Shariatmadar Tehrani F., Jamali M. High photocatalytic WO₃ nanoparticles synthesized using Sol-gel method at different stirring times. *Opt. Quantum Electron.*, 2023, **55**(3), P. 250.
- [14] Huang Z., Song J., Pan L., Zhang X., Wang L., Zou J. Tungsten Oxides for Photocatalysis, Electrochemistry, and Phototherapy. *Adv. Mater.*, 2015, **27**(36), P. 5309–5327.
- [15] Dong X., Lu Y., Liu X., Zhang L., Tong Y. Nanostructured tungsten oxide as photochromic material for smart devices, energy conversion, and environmental remediation. *J. Photochem. Photobiol. C Photochem. Rev.*, 2022, **53**, P. 100555.
- [16] Zeb S., Sun G., Nie Y., Xu H., Cui Y., Jiang X. Advanced developments in nonstoichiometric tungsten oxides for electrochromic applications. *Mater. Adv.*, 2021, **2**(21), P. 6839–6884.
- [17] George J.M., Antony A., Mathew B. Metal oxide nanoparticles in electrochemical sensing and biosensing: a review. *Microchim. Acta*, 2018, **185**(7), P. 358.
- [18] Can F., Courtois X., Duprez D. Tungsten-Based Catalysts for Environmental Applications. *Catalysts*, 2021, **11**(6), P. 703.
- [19] Kameneva S.V., Popkov M.A., Tronev I.V., Kottsov S.Y., Sozarukova M.M., Ivanov V.K. Photochromic aerogels based on cellulose and chitosan modified with WO₃ nanoparticles. *Nanosyst. Physics., Chem., Math.*, 2022, **13**(4), P. 404–413.
- [20] Staerz A., Somacescu S., Epifani M., Russ T., Weimar U., Barsan N. WO₃ Based Gas Sensors. In: *EUROSENSORS 2018*. MDPI, 2019, P. 826.
- [21] Zhou Y., She X., Wu Q., Xiao J., Peng T. Monoclinic WO₃ nanosheets-carbon nanotubes nanocomposite based electrochemical sensor for sensitive detection of bisphenol A. *J. Electroanal. Chem.*, 2022, **915**, P. 116355.
- [22] Anithaa A.C., Lavanya N., Asokan K., Sekar C. WO₃ nanoparticles based direct electrochemical dopamine sensor in the presence of ascorbic acid. *Electrochim. Acta*, 2015, **167**, P. 294–302.
- [23] Sharma A., Saini A.K., Kumar N., et al. Methods of preparation of metal-doped and hybrid tungsten oxide nanoparticles for anticancer, antibacterial, and biosensing applications. *Surfaces and Interfaces*, 2022, **28**, P. 101641.
- [24] Bashir A., Khan S.R., Aqib A.I., Shafique L., Ataya F.S. Multifunctional integration of tungsten oxide (WO₃) coating: A versatile approach for enhanced performance of antibiotics against single mixed bacterial infections. *Microb. Pathog.*, 2024, **189**, P. 106571.
- [25] Popov A.L., Han B., Ermakov A.M., et al. PVP-stabilized tungsten oxide nanoparticles: pH sensitive anti-cancer platform with high cytotoxicity. *Mater. Sci. Eng. C*, 2020, **108**, P. 110494.
- [26] Jiang X., Liu W., Li Y., et al. WO₃ nanosheets with peroxidase-like activity and carbon dots based ratiometric fluorescent strategy for xanthine oxidase activity sensing and inhibitor screening. *Talanta*, 2024, **267**, P. 125129.
- [27] Sadashivanna R.H., Krishna H., Shivakumar A., Gangadhara N.Y., Mahesh Lohith K.S., Krishnegowda A. Oxalic acid capped tungsten oxide nanozyme mimicking peroxidase activity, its synthesis characterization, and kinetic data validation via spectrophotometric studies. *Nano-Structures & Nano-Objects*, 2024, **40**, P. 101340.
- [28] Robert A., Meunier B. How to Define a Nanozyme. *ACS Nano*, 2022, **16**(5), P. 6956–6959.
- [29] Zandieh M., Liu J. Nanozymes: Definition, Activity, and Mechanisms. *Adv. Mater.*, 2024, **36**(10), P. 2211041.
- [30] Popov A.L., Savintseva I.V., Popova N.R., et al. PVP-stabilized tungsten oxide nanoparticles (WO₃) nanoparticles cause hemolysis of human erythrocytes in a dose-dependent manner. *Nanosyst. Physics., Chem., Math.*, 2019, **10**(2), P. 199–205.
- [31] Basha M.A.F. Magnetic and optical studies on polyvinylpyrrolidone thin films doped with rare earth metal salts. *Polym. J.*, 2010, **42**(9), P. 728–734.
- [32] Pacheco M.L., Pinto T.V., Sousa C.M., et al. Tuning the Photochromic Properties of WO₃-Based Materials toward High-Performance Light-Responsive Textiles. *ACS Appl. Opt. Mater.*, 2023, **1**(8), P. 1434–1451.
- [33] Hussain M., Kalulu M., Ahmad Z., Ejeromedoghene O., Fu G. Rapid fabrication of polyoxometalate-enhanced photo responsive films from ethyl cellulose (EC) and polyvinylpyrrolidone (PVP). *Int. J. Biol. Macromol.*, 2024, **280**, P. 136051.
- [34] Jiang B., Duan D., Gao L., et al. Standardized assays for determining the catalytic activity and kinetics of peroxidase-like nanozymes. *Nat. Protoc.*, 2018, **13**(7), P. 1506–1520.
- [35] Zheng J.J., Zhu F., Song N., et al. Optimizing the standardized assays for determining the catalytic activity and kinetics of peroxidase-like nanozymes. *Nat. Protoc.*, 2024, **19**, 3470–3488.
- [36] Feng K., Wang G., Wang S., et al. Breaking the pH Limitation of Nanozymes: Mechanisms, Methods, and Applications. *Adv. Mater.*, 2024, **36**(31), P. 2401619.
- [37] Eroi S.N., Ello A.S., Diabaté D., Ossoonon D.B. Heterogeneous WO₃/H₂O₂ system for degradation of Indigo Carmin dye from aqueous solution. *South African J. Chem. Eng.*, 2021, **37**, P. 53–60.

- [38] Shi R., Wei S., Cheng S., Zeng J., Wang Y., Shu X. Colorimetric Detection of Glucose Using WO₃ Nanosheets as Peroxidase-mimetic Enzyme. *Chem. Res. Chinese Univ.*, 2022, **38**(4), P. 985–990.
- [39] Yang J., Cheng S.Q., Shi R., Ying Qin S., Huang L., Lin Wang Y. Spectrophotometric detection of uric acid with enzyme-like reaction mediated 3,3',5,5'-tetramethylbenzidine oxidation. *Bull. Chem. Soc. Ethiop.*, 2022, **37**(1), P. 11–21.
- [40] Li Z., Liu X., Liang X.H., Zhong J., Guo L., Fu F. Colorimetric determination of xanthine in urine based on peroxidase-like activity of WO₃ nanosheets. *Talanta*, 2019, **204**, P. 278–284.

Submitted 25 October 2024; accepted 12 November 2024

Information about the authors:

Matvei A. Popkov – Kurnakov Institute of General and Inorganic Chemistry, Russian Academy of Sciences, Leninsky, 31, Moscow, 119991, Russia; ORCID 0000-0002-9811-6241; ma_popkov@igic.ras.ru

Ekaterina D. Sheichenko – Kurnakov Institute of General and Inorganic Chemistry, Russian Academy of Sciences, Leninsky, 31, Moscow, 119991, Russia; HSE University, Myasnitskaya, 20, Moscow, 101000, Russia; ORCID 0000-0003-3485-1842; edsheychenko@edu.hse.ru

Arina D. Filippova – Kurnakov Institute of General and Inorganic Chemistry, Russian Academy of Sciences, Leninsky, 31, Moscow, 119991, Russia; ORCID 0000-0002-2725-8891; arifilippova@yandex.ru

Ilya V. Tronev – Kurnakov Institute of General and Inorganic Chemistry, Russian Academy of Sciences, Leninsky, 31, Moscow, 119991, Russia; ORCID 0000-0002-0718-1911; ivtronev@edu.hse.ru

Kristina N. Novoselova – Kurnakov Institute of General and Inorganic Chemistry, Russian Academy of Sciences, Leninsky, 31, Moscow, 119991, Russia; HSE University, Myasnitskaya, 20, Moscow, 101000, Russia; ORCID 0009-0006-4139-1476; knnovoselova@edu.hse.ru

Evelina A. Trufanova – Kurnakov Institute of General and Inorganic Chemistry, Russian Academy of Sciences, Leninsky, 31, Moscow, 119991, Russia; HSE University, Myasnitskaya, 20, Moscow, 101000, Russia; ORCID 0009-0009-1645-5759; eatrufanova_1@edu.hse.ru

Darya N. Vasilyeva – Kurnakov Institute of General and Inorganic Chemistry, Russian Academy of Sciences, Leninsky, 31, Moscow, 119991, Russia; HSE University, Myasnitskaya, 20, Moscow, 101000, Russia; ORCID 0009-0004-3560-4178; dnvasileva_1@edu.hse.ru

Maria R. Protsenko – Kurnakov Institute of General and Inorganic Chemistry, Russian Academy of Sciences, Leninsky, 31, Moscow, 119991, Russia; HSE University, Myasnitskaya, 20, Moscow, 101000, Russia; ORCID 0009-0007-0738-4974; mrprotsenko@edu.hse.ru

Madina M. Sozarukova – Kurnakov Institute of General and Inorganic Chemistry, Russian Academy of Sciences, Leninsky, 31, Moscow, 119991, Russia; ORCID 0000-0002-5868-4746; s_madinam@bk.ru

Alexander E. Baranchikov – Kurnakov Institute of General and Inorganic Chemistry, Russian Academy of Sciences, Leninsky, 31, Moscow, 119991, Russia; HSE University, Myasnitskaya, 20, Moscow, 101000, Russia; ORCID 0000-0002-2378-7446; a.baranchikov@yandex.ru

Vladimir K. Ivanov – Kurnakov Institute of General and Inorganic Chemistry, Russian Academy of Sciences, Leninsky, 31, Moscow, 119991, Russia; HSE University, Myasnitskaya, 20, Moscow, 101000, Russia; ORCID 0000-0003-2343-2140; van@igic.ras.ru

Conflict of interest: the authors declare no conflict of interest.